THE ASTROPHYSICAL JOURNAL, 556:970–978, 2001 August 1


# THERMAL EQUILIBRATION OF $^{26}$Al

R. C. RUNKLE,[1] A. E. CHAMPAGNE,[1] AND J. ENGEL
Department of Physics and Astronomy, University of North Carolina, Chapel Hill, Chapel Hill, NC 27599-3255
*Received 2000 September 6; accepted 2001 April 2*

## ABSTRACT

In astrophysical environments, the long-lived ($t_{1/2} = 0.72$ Myr) ground state of $^{26}$Al can communicate with its short-lived ($t_{1/2} = 6.35$ s) first excited state through thermal excitations. The result is that the astrophysical half-life for $^{26}$Al can be much shorter than the laboratory value, which can have an impact on the amount of $^{26}$Al produced at high temperatures. We have reexamined the equilibration process using the results of new calculations of some of the key transition rates. In addition, we discuss a simple way of describing the behavior of $^{26}$Al in a stellar plasma and use this to better define the conditions where equilibration is expected to be important. Finally, we present a series of network calculations to show how the interplay between the timescale for equilibration versus that for nuclear reactions will govern the evolution of $^{26}$Al.

*Subject headings:* nuclear reactions, nucleosynthesis, abundances — stars: abundances

## 1. INTRODUCTION

Measurements and observations have provided clear evidence for the presence of $^{26}$Al in the early solar system and in the present interstellar medium. The ground state of $^{26}$Al decays via positron emission ($\beta^+$) and electron capture to $^{26}$Mg with a half-life of $t_{1/2} = 0.72$ Myr; the signature for $^{26}$Al in the interstellar medium is the characteristic 1809 keV gamma ray that is emitted subsequent to this decay. Maps of this emission show a rather lumpy distribution, qualitatively consistent with episodic production from massive stars (see, e.g., the review of Prantzos & Diehl 1996). However, some of the emission features may be numerical artifacts (Knödlseder et al. 1999). Although massive stars are still favored (Knödlseder 1999), it has not been possible to uniquely identify the specific source(s) responsible or even the requisite astrophysical conditions for $^{26}$Al production. Clearly work remains to be done on the theoretical and observational sides of this problem, but there are also deficiencies in the relevant nuclear physics that need to be addressed.

In addition to the ground-state decay, the first excited state of $^{26}$Al at $E_x = 228$ keV undergoes a superallowed $\beta^+$ transition to the ground state of $^{26}$Mg with a half-life of $t_{1/2} = 6.35$ s. Gamma decay between this isomer and the ground state is severely hindered by their large spin difference ($\Delta J = 5$). However, if this state were effectively linked to the ground state through thermal excitations involving other excited states, then the astrophysical half-life of $^{26}$Al would be reduced from its laboratory value. This effect was examined in detail by Ward & Fowler (1980, hereafter WF). One important result from that work was that the abundance ratio of isomer to ground state would not reach the thermal equilibrium value for temperatures below $T \approx 0.4$ gK ($T_9 \approx 0.4$). From this they concluded that the ground state and isomer would evolve as "separate" (i.e., physically distinct) nuclei rather than as states of the same nucleus. However, by their own admission, WF used crude approximations for some important gamma-ray transition rates. The rates were calculated more carefully by Coc, Porquet, & Nowacki (1999, hereafter CPN), who focused on the onset of equilibrium during novae. Although they also conclude that the ground state and isomer behave as separate nuclei for $T_9 < 0.4$, their calculation of the effective lifetime of $^{26}$Al for these temperatures clearly shows that the isomer and ground state do communicate. In this sense, the notion of separate nuclei refers to how these two states are described within a reaction network. The inference is that while they may be entered as separate nuclei, the correct effective decay rate would have to be employed as well.

In this paper, we extend this discussion to higher temperatures. In addition, we will develop some simple criteria to assess the importance of equilibration in calculations of nucleosynthesis. We will also show that the question of separate nuclei versus equilibrated states will depend on relevant timescales as well as on temperature. The concept of quasi-equilibrium, not considered explicitly by WF, will also be important here.

## 2. INPUT PHYSICS

### 2.1. *Gamma-Ray Rates*

In general, the ground state of $^{26}$Al may make transitions to excited states by absorption of photons or by interactions with electrons and ions. Similarly, deexcitation of an excited state may be stimulated by photons or particles. In certain environments, the particle interactions may dominate, but only when equilibrium would be quickly reached even without their presence. Therefore, particle processes are never of much practical significance, and we restrict our attention to gamma rays.

The basic approach to calculating the behavior of $^{26}$Al in a photon bath has been described by WF. Briefly, the transition rate linking an initial state $i$ with a higher lying final state $f$ is

$$\lambda_{if} = \frac{g_f}{g_i} \frac{\lambda_s}{e^{E_{if}/kT} - 1}, \quad (1)$$

where $g = 2J + 1$, $\lambda_s$ is the rate for spontaneous decay from $f$ to $i$, $E_{if}$ is the energy difference between $i$ and $f$, and $k$ is Boltzmann's constant. The corresponding total decay rate between $i$ and $f$ (including stimulated emission) is

$$\lambda_{if} = \frac{\lambda_s}{1 - e^{-E_{if}/kT}}. \quad (2)$$

[1] Triangle Universities Nuclear Laboratory, Duke University, Durham, NC 27708-0308.

Since the levels of $^{26}$Al have been studied in great detail, the spontaneous decay rates can in principle be obtained from the known lifetimes and decay schemes (Endt 1990). However, branching ratios below $10^{-3}$ are difficult to measure, and so some weak gamma transitions have gone unrecorded. For example, the $E_x = 417$ keV state is observed to decay via an E2 transition to the ground state (Fig. 1), but the weak M3 transition to the isomer has never been observed. A comparable situation exists in the case of the third excited state (at $E_x = 1058$ keV). This state has a measured 100% M1 branch to the isomer, so the weak E2 transition to the state at $E_x = 417$ keV has escaped detection. Single-particle estimates for these two weak transitions were made by WF. Although at first glance these transitions do not seem important, they are in fact the primary routes to equilibration for $T_9 \leq 1.5$. Other weak gamma decays involving states at higher excitation energies should exist, but at stellar temperatures the low-lying states are predominantly populated.

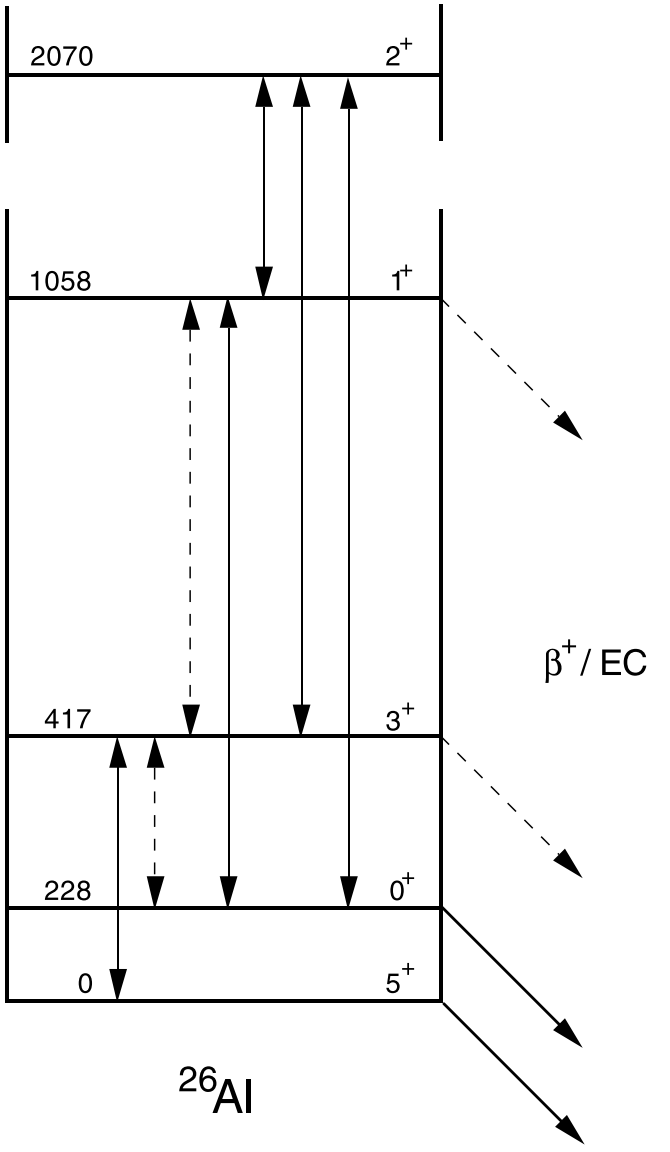


FIG. 1.—Levels and transitions that play a role in the equilibration of $^{26}$Al for $T_9 \leq 5$; energies are in keV. Solid lines represent transitions where the corresponding decay has been observed; dashed lines denote calculated transitions.

WF warned that their calculations of the weak transitions most likely overestimate the actual decay rates, and CPN performed shell-model calculations to obtain more reliable values. Since $^{26}$Al resides in the well-studied *sd*-shell ($A = 17$–$39$), where theoretical predictions are usually successful, such calculations should be an improvement over single-particle estimates. However, because these transitions are most likely unmeasureable, some estimate of the reliability of the theoretical results is warranted. To do this, we have calculated transition rates in $^{26}$Al using the shell model. Although our calculation differs from that of CPN in several respects, both employ the Wildenthal USD interaction (Wildenthal 1984) and $0d_{5/2}$–$1s_{1/2}$–$0d_{3/2}$ basis. The use of this interaction is justified on the grounds that it is derived from fits of spectroscopic data in the *sd*-shell and is therefore expected to provide accurate transition matrix elements, at least for the lower order multipoles. These matrix elements, $M(f, i)$, were calculated with the code *oxbash* (Brown, Etchegoyen, & Rae 1988) and are related to the E2 and M3 transition probabilities $B$ via

$$B = \frac{[M(f, i)]^2}{2J_i + 1}, \tag{3}$$

where $J_i$ is the spin of the initial state. Previous work demonstrates that restriction to an *sd*-basis requires the use of effective charges and $g$-factors. The effective charges used here are $1.35e$ and $0.35e$ for $e_p$ and for $e_n$, respectively, as suggested by Carchidi, Wildenthal, & Brown (1986). CPN used a slightly different prescription, but this turns out to have a small effect on the E2 transition rates. To gain a feeling for the reliability of these results, we have calculated the E2 rates for all of the known transitions in $^{26}$Al up to $E_x = 3073$ keV. These rates (listed in Table 1) generally reproduce the experimental values. However, this is not true for transitions from the 2365 and 2545 keV states, where the shell model overpredicts the experimental values by a factor of 5–10. A weighted average of the ratio of the observed rates to the predictions is 0.43 (5), and we adopt a symmetric uncertainty corresponding to $\sigma_\lambda/\lambda = 0.6$ as a measure of the theoretical uncertainty for the $1058 \rightarrow 0$ transition rate. Unlike CPN, we do not consider the agreement between theory and experiment for the other multipolarities because the respective operators are different and constrain the shell-model interaction in different ways.

There are fewer data on M3 transitions, so the corresponding effective $g$-factors are harder to infer. Brown et al. (1980) arrived at an effective spin $g$-factor of 0.87 after empirically fitting measured transitions in $A = 24$, 34, and 38. Their result is supported by an analysis of second forbidden $\beta$-decay by Warburton (1992), and it is what we use here. CPN used a different prescription. In both cases, the predicted rates are larger than the experimental values, but the present approach seems to do a better job of reproducing the experimental rates. Unfortunately, this comparison is restricted to just the three known transitions in $A = 24$ and 34 that can be calculated "reliably" (Brown et al. 1980), and this does not provide a large basis for comparison. However, it does seem that the $417 \rightarrow 228$ rate is probably accurate to a factor of 2–3.

Our results and those of CPN are listed in Table 1 and the agreement for the two transitions of interest is quite good. In this sense, it can be argued that these calculations are robust, but the agreement is primarily a result of the fact

TABLE 1

LABORATORY ELECTROMAGNETIC TRANSITION RATES

| TRANSITION | MULTIPOLARITY | $\lambda_{if}$ ($s^{-1}$) This Study | $\lambda_{if}$ ($s^{-1}$) CPN | $\lambda_{if}$ ($s^{-1}$) Literature[a] |
|---|---|---|---|---|
| 417 → 0 ..... | E2 | $6.88 \times 10^{8}$ | $7.41 \times 10^{8}$ | $5.56(15) \times 10^{8}$ |
| 417 → 228 ..... | M3 | 0.062 | 0.065 | ... |
| 1058 → 417 ..... | E2 | $7.24 \times 10^{8}$ | $7.67 \times 10^{8}$ | ... |
| 1850 → 417 ..... | E2 | $3.13 \times 10^{11}$ | ... | $1.52(27) \times 10^{11}$ |
| 2069 → 228 ..... | E2 | $1.35 \times 10^{12}$ | ... | $1.50(30) \times 10^{12}$ |
| 2072 → 417 ..... | E2 | $1.62 \times 10^{11}$ | ... | $2.00(41) \times 10^{11}$ |
| 2365 → 0..... | E2 | $6.50 \times 10^{10}$ | ... | $6.36(139) \times 10^{9}$ |
| 2545 → 0..... | E2 | $1.21 \times 10^{10}$ | ... | $2.10(80) \times 10^{9}$ |
| 2545 → 1058..... | E2 | $1.12 \times 10^{11}$ | ... | $2.50(66) \times 10^{10}$ |
| 2740 → 417 ..... | E2 | $4.18 \times 10^{11}$ | ... | $1.86(51) \times 10^{11}$ |
| 3073 → 0..... | E2 | $2.13 \times 10^{10}$ | ... | $2.82(56) \times 10^{10}$ |
| 3073 → 1058..... | E2 | $3.31 \times 10^{11}$ | ... | $4.39(72) \times 10^{11}$ |
| 3073 → 1850..... | E2 | $6.89 \times 10^{10}$ | ... | $9.61(157) \times 10^{10}$ |

[a] Endt (1990).

that the same interactions were used in both cases. A better test of reliability is the comparison with experiment, as described above.

### 2.2. *Weak Decays*

At high temperatures and densities, a sizeable fraction of $^{26}$Al exists in excited states. Therefore it is important to consider the $\beta^+$ and electron-capture decays from these states as well as those from the ground state and isomer. Since these transitions are not observable in the laboratory, their rates must be calculated. As will become clear in § 3, the important decays are the Gamow-Teller transitions from the 417 keV state to the 1809 keV state in $^{26}$Mg and from the 1058 keV state to both ground and 1809 keV states. The strength of the 417 → $^{26}$Mg (1809) transition was estimated by WF, who assigned $\log ft = 5.3$. Shell-model calculations of these transitions have been carried out by Kajino et al. (1988), again using the Wildenthal interaction. Our calculations yield transition rates that differ from these by only 5%–10%. One important point is that the decay rate for the 1058 keV state is comparable to that of the isomer. For temperatures at which the thermal population of this state is significant, its decay will influence the total decay rate. However, since the effective decay rate for $T_9 \leq 5$ is still dominated by the decay of the isomer, the theoretical uncertainties associated with the calculated rates have a negligible impact on calculations of equilibration, and we ignore them here.

## 3. THE BEHAVIOR OF $^{26}$Al IN A STELLAR PLASMA

Although the equilibration of $^{26}$Al is best treated within the framework of a detailed network calculation, some insight into the process itself can be gained from a simple analytic approximation. Two situations were discussed by WF: direct equilibration between two levels and equilibration through intermediate states. The case of $^{26}$Al was considered within the framework of the latter process. Although their description of equilibration through an intermediate state is correct in a general sense, it does not describe the particular case of $^{26}$Al, which behaves as a system of two quasi-equilibrium clusters. One cluster includes the ground state and those states that communicate rapidly with the ground state. The other involves the isomer and its group of states. Equilibrium *within* each cluster is reached very quickly. In contrast, the links connecting these clusters are comparatively slow, and therefore equilibrium *between* the clusters is reached at a much later time. For example, at $T_9 = 0.3$–5, the isomer will equilibrate with the 1058 keV state with a time constant of 40 to 20 fs, whereas the time constant for equilibration with the ground state is 3100–$7.5 \times 10^{-11}$ s. Thus, the internal equilibration within a cluster is effectively instantaneous. In this approximation, equilibration between clusters is analogous to equilibration within a two-level system.

We will consider the simplest case, in which the ground-state cluster is just the ground state and the 417 keV state and the isomer cluster contains only the isomer and 1058 keV state. Other excited states clearly come into play as the temperature is increased. Nonetheless, this crude approximation contains the essential physics and reproduces the asymptotic behavior of the system. Within this simple model, we will focus on the internal behavior of the system (equilibration) and ignore external factors (nuclear reactions other than $\beta$-decay). Then the time evolution of the clusters can be written as

$$\frac{d}{dt}(n_0 + n_2) = -n_0\lambda_\beta^0 - n_2(\lambda_{2m} + \lambda_{23} + \lambda_\beta^2) + n_m\lambda_{m2} + n_3\lambda_{32}\,, \quad (4)$$

$$\frac{d}{dt}(n_m + n_3) = -n_m(\lambda_\beta^m + \lambda_{m2}) - n_3(\lambda_{32} + \lambda_\beta^3) + n_2(\lambda_{2m} + \lambda_{23})\,, \quad (5)$$

where the subscripts 0, $m$, 2, and 3 refer to the ground state, isomer, 417 keV, and 1058 keV states, respectively. The electromagnetic transition rates for $i \rightarrow f$ are denoted as before by $\lambda_{if}$ and the $\beta$-decay rates for the $i$th states by $\lambda_\beta^i$. The abundance of the $i$th state is written as $n_i$. These expressions can be rewritten in terms of $n_0$ and $n_m$ as

$$\frac{d}{dt}(1 + c_{20})n_0 = -n_0[\lambda_\beta^0 + c_{20}(\lambda_{2m} + \lambda_{23} + \lambda_\beta^2)] + n_m(\lambda_{m2} + c_{3m}\lambda_{32})\,, \quad (6)$$

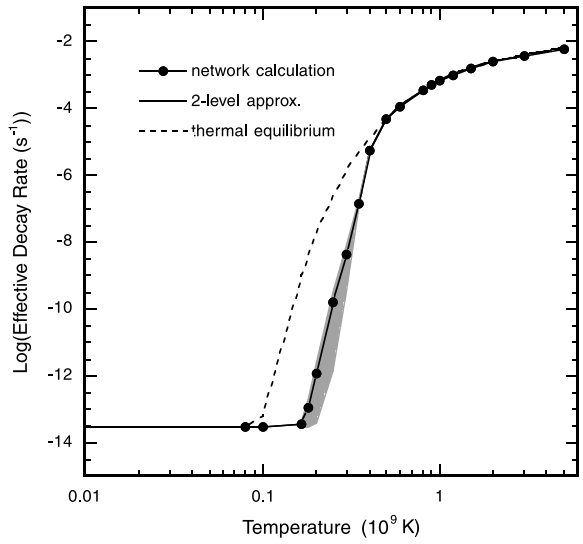


FIG. 2.—Effective decay rate as a function of temperature. Solid line was calculated using the two-level approximation; dots are the results of network calculations; shaded region denotes the 1 $\sigma$ range of uncertainty; dashed line is arrived at by assuming that the ground state and isomer are in thermal equilibrium.

$$\frac{d}{dt}(1 + c_{3m})n_m = -n_m[\lambda_\beta^m + \lambda_{m2} - c_{3m}(\lambda_{32} + \lambda_\beta^3)] + n_0\, c_{20}(\lambda_{2m} + \lambda_{23})\,. \tag{7}$$

The factors $c_{ij}$ are the thermal equilibrium abundance ratios

$$c_{ij} = \frac{g_i}{g_j}\, e^{-(E_{xi} - E_{xj})/kT}\,. \tag{8}$$

This can be recast in the form of a matrix equation

$$\frac{d}{dt}\boldsymbol{N} = \boldsymbol{T}\cdot\boldsymbol{N}\,, \tag{9}$$

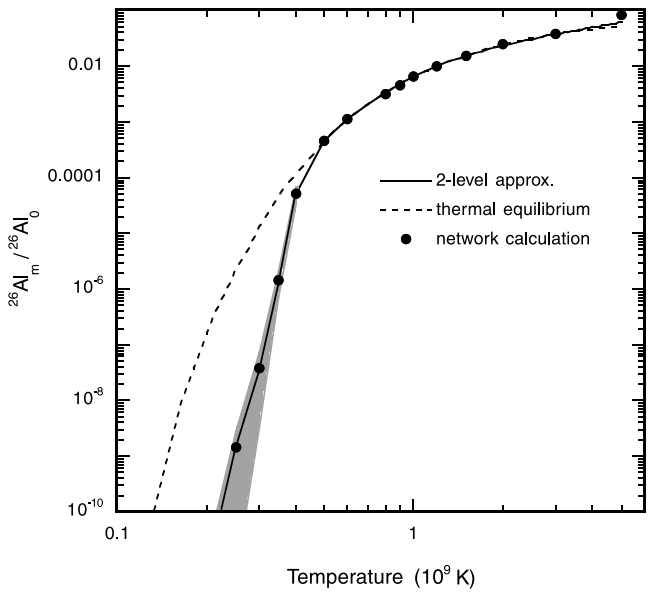


FIG. 3.—Asymptotic ratio of isomer to ground state calculated using the two-level approximation (*solid line*) and assuming thermal equilibrium (*dashed line*). Dots are the results of network calculations and the shaded region denotes the 1 $\sigma$ range of uncertainty.

where $\boldsymbol{T}$ is the transition matrix that follows from equations (4) and (5), and

$$\boldsymbol{N} = \begin{Bmatrix}(1 + c_{20})n_0(t)\\ (1 + c_{3m})n_m(t)\end{Bmatrix}. \tag{10}$$

The general solution to this equation is of the form

$$\boldsymbol{N}(t) = \boldsymbol{N}_1\, e^{-\lambda_1 t} + \boldsymbol{N}_2\, e^{-\lambda_2 t}\,, \tag{11}$$

where $\boldsymbol{N}_i$ and $-\lambda_i$ are the eigenvectors (normalized to the correct initial abundances) and eigenvalues of $\boldsymbol{T}$, respectively. The eigenvalues are

$$\lambda_1 \approx \frac{c_{20}(\lambda_{2m} + \lambda_{23})}{1 + c_{20}} + \frac{\lambda_{m2} + \lambda_\beta^m + c_{3m}(\lambda_{32} + \lambda_\beta^3)}{1 + c_{3m}}\,, \tag{12}$$

$$\lambda_2 \approx \frac{\lambda_\beta^0}{1 + c_{20}} + \frac{c_{20}(\lambda_\beta^m + c_{3m}\lambda_\beta^3)}{1 + c_{20}} \times \frac{\lambda_{2m} + \lambda_{23}}{\lambda_\beta^m + \lambda_{m2} + c_{3m}(\lambda_\beta^3 + \lambda_{32})}\,. \tag{13}$$

These approximations are valid for $T_9 \le 5$. Throughout this temperature range $\lambda_1 \gg \lambda_2$, and hence for sufficiently long times

$$\boldsymbol{N}(t) \approx \boldsymbol{N}_2\, e^{-\lambda_2 t}\,. \tag{14}$$

This is the general condition for equilibrium in a case such as this where the total number of nuclei diminishes with time. The decay rate $\lambda_2$ is thus the effective decay rate of the equilibrated nucleus. This is shown in Figure 2 along with the rate derived from network calculations. Our simple approximation reproduces the network results to within a standard deviation of 2.7% despite the fact that we have ignored the higher lying excited states. This is because the additional states mainly affect the time required to reach equilibrium. Although the $\beta$-decays from higher lying states must influence the effective decay rate at some level, the relative population of these states is small compared to the states that we have included here.

It is important to note that equilibrium or quasi-equilibrium will eventually be established at *any* temperature, including low temperatures where the equilibration time is longer than the lifetime of the isomer. However, the abundance ratio of the isomer to the ground state need not follow that of an isolated system in thermal equilibrium. Nuclear reactions and $\beta$-decays can lead to a quasi-equilibrium with nonthermal abundance patterns. In the case of full thermal equilibrium, the ratio of isomer to ground state is described by

$$\frac{n_m}{n_0} = \frac{g_m}{g_0}\, e^{-E_x(m)/kT} = \frac{1}{11}\, e^{-2.646/T_9}\,. \tag{15}$$

This should be compared to the ratio derived from our two-level approximation,

$$\frac{n_m}{n_0} = \frac{c_{20}(\lambda_{2m} + \lambda_{23})}{(1 + c_{3m})\lambda_2 + \lambda_\beta^m + \lambda_{m2} + c_{3m}(\lambda_\beta^3 + \lambda_{32})} \approx \frac{c_{20}(\lambda_{2m} + \lambda_{23})}{\lambda_\beta^m + \lambda_{m2} + c_{3m}(\lambda_\beta^3 + \lambda_{32})}\,, \tag{16}$$

which is displayed in Figure 3. The latter does a much better job of reproducing the network results at low temperatures, where the deviation from thermal equilibrium is significant.

This deviation was the criterion used by WF to differentiate between descriptions of the ground state and isomer as an equilibrating system with thermal populations ($T_9 > 0.4$) versus separate nuclei ($T_9 \leq 0.4$). However, we will show below that a thermal population distribution is reached only if nuclear reactions are sufficiently slow that the system can evolve on a timescale set by equilibration. Otherwise, quasi-equilibrium behavior will be displayed.

## 4. NETWORK CALCULATIONS

### 4.1. *Constructing the Network*

In order to examine how $^{26}$Al progresses toward equilibrium, we must first construct the set of coupled first-order equations that describe the time evolution of the states in $^{26}$Al. To start, we have included all of the excited states below $E_x = 3$ MeV. Our first goal is to calculate the timescale for equilibration, so we will ignore the states in $^{26}$Mg populated by weak transitions as well as production and destruction via $(p, \gamma)$ reactions. The resulting network includes 14 states and 82 independent gamma transitions linking these states. In the case of no destruction, the time constant for equilibration $\tau_{eq}$ is the inverse of the smallest eigenvector of $\boldsymbol{T}$, i.e., the longest time constant of the system. There is some confusion regarding this point in WF, but their plot of $\tau_{eq}$ is consistent with this definition. Since the rates for the $417 \rightarrow 228$ and $1058 \rightarrow 0$ transitions have been reduced by factors of 6.7 and 3.2, respectively, $\tau_{eq}$ is increased as compared with the results of WF for $T_9 \leq 1.8$, as shown in Figure 4. For example, for $T_9 = 0.3$–1.0, this increase is a factor of 7.6 to 2.9. However, to reiterate a point made by WF, a time longer than $\tau_{eq}$ will pass before equilibrium behavior manifests itself. For the sake of illustration, we will arbitrarily define this time as the time required for the abundances to evolve to within 1% of their values at $t = \infty$. As is apparent in Figure 4, this time is substantially longer than $\tau_{eq}$.

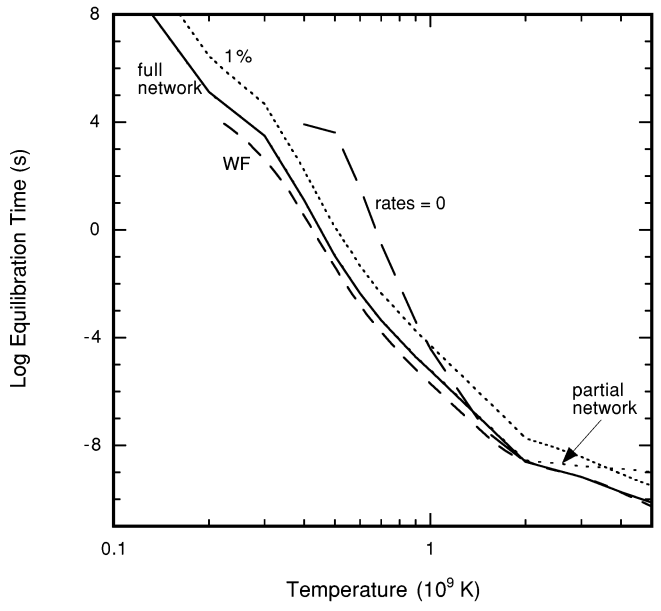


FIG. 4.—Time required for the ground state and isomer to reach equilibrium vs. temperature. Curve labeled *full network* refers to the inverse of the smallest eigenvalue of the transition matrix for the full network of equilibrating transitions. Curves labeled "partial network," "rates = 0," and "WF" are the same quantity calculated for the truncated network (described in the text) when the rates of the weak gamma branches are set to zero and with the rates from WF, respectively. Curve labeled "1%" is the time required for $m/g$ to come within 1% of the equilibrium ratio.

Unfortunately, 82 links represent a significant overhead to pay in more general nucleosynthesis calculations, and therefore we present a pared-down network that preserves the behavior of the system. The states that we include are the ground state, the isomer, and the $E_x = 417$, 1058, 2069, 2070, and 2072 keV states. The number of links is then reduced to 28. This reduced network will overpredict the time required to reach equilibrium (e.g., by about 25% for $T_9 = 2$–5), but this is a small amount compared to the time over which the stellar burning occurs. Since the latter three states are nearly degenerate, it is tempting to treat them as a single effective state, thereby further simplifying the network. However, these states have very different decay schemes. Ignoring the two decays that we have calculated, the 2069 keV state will cascade only to the ground state, whereas the 2072 keV state ultimately populates just the isomer. In contrast, the 2070 keV state has decays that terminate in both the ground state and isomer. If all of these transitions were to be ascribed to a single state, there would be spurious links between the ground state and isomer and the equilibrium abundance ratios would be in error. We choose instead to neglect the 2069 and 2072 keV states. This means that the predicted onset of equilibrium is further delayed; but again, in terms of the timescales relevant to stellar burning, the delay is not important. Our final network contains 14 transitions linking the five remaining states. These five were also the states judged by WF as the most important equilibration process.

### 4.2. *Results*

#### 4.2.1. $\tau_{eq} \geq \tau_{\beta}$

In a simple thermal equilibrium, the ratio of isomer to ground state is always less than 0.091, and so equilibration can act to enhance the ground state at the expense of the isomer if the production ratio $m/g$ is greater then the equilibrium ratio. However, this general behavior is modified by the fact that both states can $\beta$-decay. Figure 5 shows the time evolution of the ground state and isomer, calculated with our truncated network for $T_9 = 0.3$, a temperature

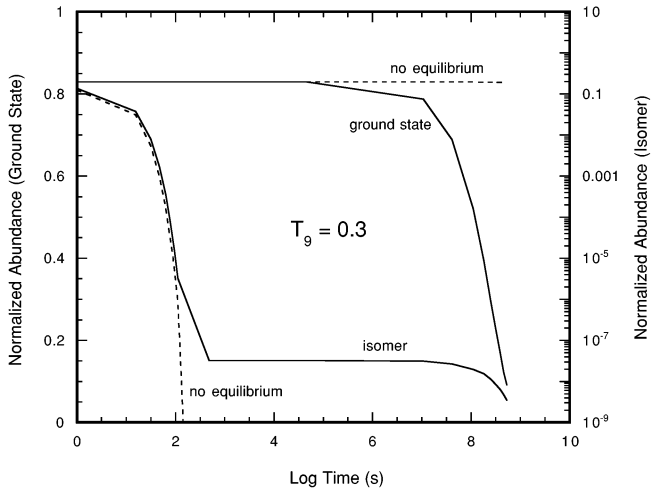


FIG. 5.—Network calculations showing the evolution of the ground state and isomer for $T_9 = 0.3$. The total initial abundance is normalized to unity. Curves labeled "no equilibrium" represent the abundances calculated with the rates of the equilibrating transitions set to zero.

where the equilibration time is longer than the lifetime of the isomer. We still ignore any nuclear reactions that absorb or emit particles. The relative initial abundances are given by the fraction of time that the $^{25}$Mg($p$, $\gamma$) reaction populates the ground state versus the isomer. Since $\tau_{eq} \geq \tau_\beta$, it is tempting to suppose that the system will not reach equilibrium. In fact, quasi-equilibrium is established between the ground state and isomer, but only after the abundance of the isomer has dropped significantly from $\beta$-decay. After this point, the two states maintain a constant relative abundance that is a factor of 345 less than the thermal equilibrium value and decay with the same effective rate. This temperature is within the "separated nuclei" regime discussed by WF. However, they assumed that the primary decay mode of the ground state would be a combination of direct $\beta$-decay and $\beta$-decay of the 417 keV state following its equilibration with the ground state. Thus, at low temperatures there would not be any significant communication between the isomer and the ground state, and both states would evolve independently. Although CPN did not calculate the $\beta$-decay rate of the 417 keV state, they are correct in their assertion that the decay of the isomer primarily determines the effective decay rate of the ground state. In a physical sense, the ground state and the isomer are clearly not separated. However, they can be entered as separate nuclei in a reaction network provided that the appropriate effective decay rate is used, a point that will be discussed in more detail when we include other nuclear reactions in the network.

#### 4.2.2. $\tau_{eq} \leq \tau_\beta$

In Figures 6 and 7 we show the results of network calculations for higher temperatures, specifically $T_9 = 0.4$ (where $\tau_{eq} \approx \tau_\beta$) and 2.0 ($\tau_{eq} < \tau_\beta$). Again, we have ignored all reactions that absorb or emit particles. A basic pattern persists throughout this temperature range. Material initially flows from the isomer to the ground state. The net enhancement of the ground state is about 6%–15% throughout this temperature range. Once the system reaches equilibrium, the abundance of the ground state drops together with that of the isomer, again with an effective lifetime that is shorter than that for the ground state but longer than that of the isomer. The relative abundance of isomer to ground state reaches the thermal equilibrium value, and thus we are in the equilibration regime of WF. However, we will show in

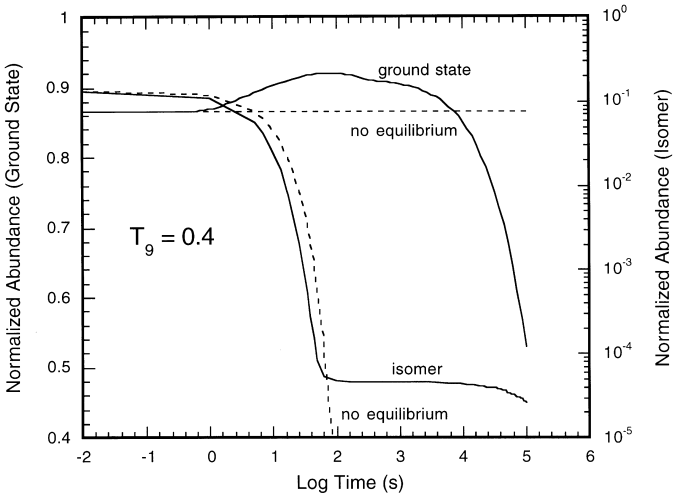


FIG. 6.—Same as Fig. 5, but for $T_9 = 0.4$

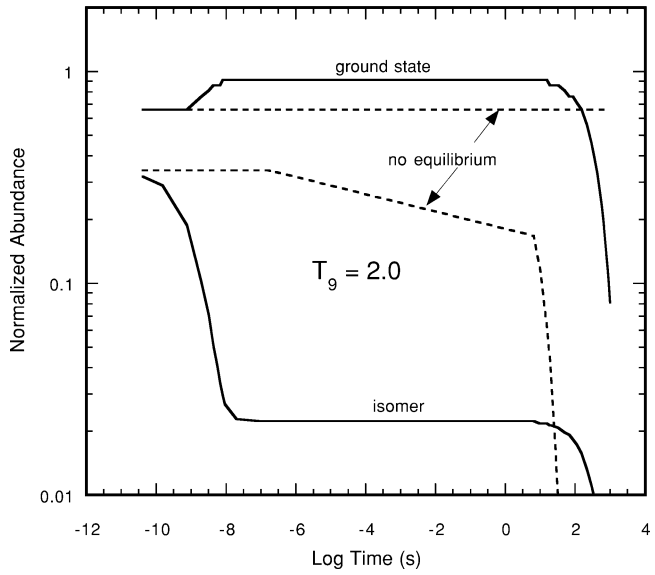


FIG. 7.—Same as Fig. 5, but for $T_9 = 2$

§ 4.2.3, where we include other nuclear reactions, that in some circumstances $^{26}$Al can still be described as two separate nuclei with effective lifetimes, even for $T_9 > 0.4$.

#### 4.2.3. *Equilibrium and Quasi-Equilibrium Behavior*

The criterion used by WF to determine whether $^{26}$Al behaves as an equilibrated system or as separate nuclei is the population ratio of isomer to ground state as $t \to \infty$. Clearly, if this ratio evolves to the thermal value, then thermal equilibrium most likely pertains. However, this choice is too restrictive in the sense that it does not account for the possibility of quasi-equilibrium behavior. The simple examples described above showed the onset of quasi-equilibrium at low temperatures, but temperature alone is not the factor that determines whether quasi or full equilibrium is appropriate. The evolution toward an equilibrated state is governed by the interplay of the timescale for equilibration $\tau_{eq}$ and the characteristic timescale for nuclear reactions or decays (including the $\beta$-decays already discussed), $\tau_{nuc}$. If $\tau_{eq} < \tau_{nuc}$, then equilibration occurs more rapidly than abundance changes from nuclear interactions. Consequently, the system will evolve to thermal equilibrium. On the other hand, if $\tau_{eq} > \tau_{nuc}$, then equilibration lags behind the faster nuclear interactions and a quasi-equilibrium ensues. Temperature and density together determine $\tau_{nuc}$, and hence it is possible to have conditions leading to quasi-equilibrium at high temperatures. This is in contrast with the accepted notion that thermal equilibrium applies for $T_9 > 0.4$.

The behavior of $^{26}$Al will also depend on the relative population of the isomer and ground state by nuclear reactions and decays. In most cases, these will preferentially produce the ground state; the production of the isomer over a wide range of temperatures is usually no more than about 10%–20% of that of the ground state. Equilibration will rearrange these abundances, usually by a flow from the isomer to the ground state (since the ratio $m/g$ at equilibrium is usually less than the production ratio). However, since equilibration will increase the absolute abundance of the ground state by at most a small amount, the primary effect of equilibration is simply to shorten the lifetime of the

ground state. The lone exception to this rule occurs when the $\beta^+$-decay of $^{26}$Si is important, as this populates only the isomer for the temperatures under consideration here. As long as $^{26}$Al is produced primarily in its ground state, it should be possible to describe equilibration by using effective decay rates, treating the internal links between the isomer and ground state implicitly.

To illustrate these points, we now consider a more complete network that includes the nuclear reactions and decays linking 140 stable and radioactive nuclei between $^1$H and $^{50}$Ti. Note that WF did not include reactions involving any short-lived nuclei in their network calculations. We used solar initial abundances under conditions of constant temperature and density. The reactions directly relevant to $^{26}$Al were taken either from the NACRE compilation (Angulo et al. 1999) or from a more recent evaluation (Iliadis et al. 2001). Figures 8, 9, and 10 show the evolution of the ground state and isomer for $T_9 = 0.3$, 1.5, and 5, respectively. The top part of each figure was calculated with a density that made the timescales for relevant $(p, \gamma)$ reactions less than $\tau_{eq}$. The bottom of each figure shows the opposite situation. In each case, the abundances were calculated both with the equilibrating transitions (*solid lines*) and with effective decay rates (*dashed lines*).

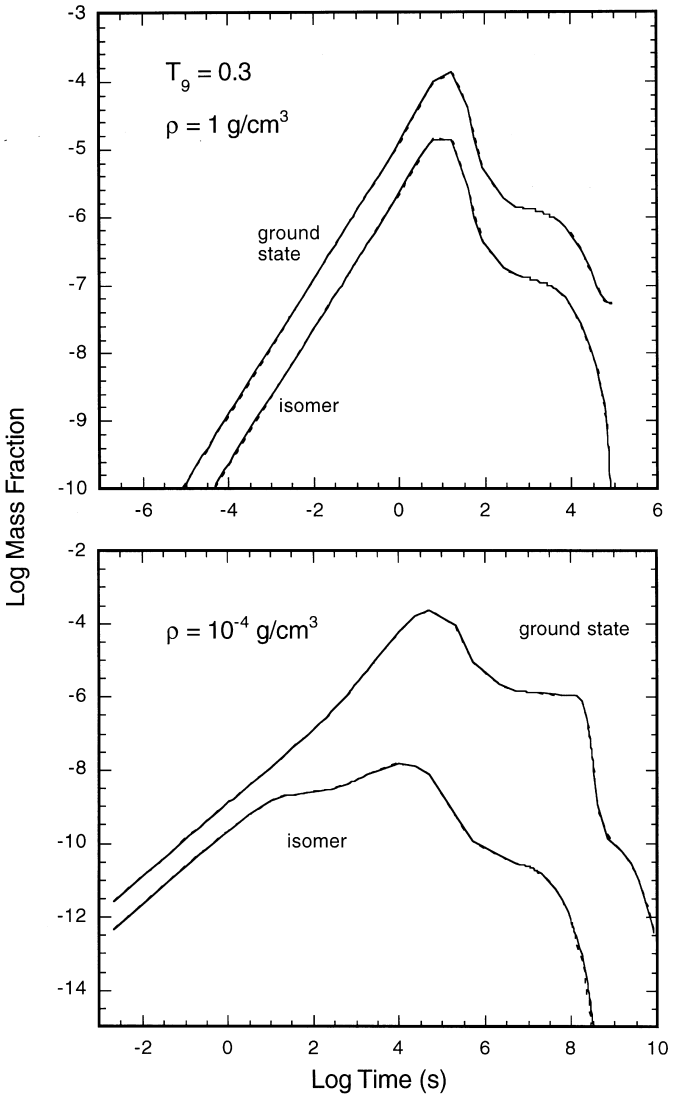


FIG. 8.—Network calculations including all nuclear interactions for $T_9 = 0.3$, and $\rho = 1 \times 10^{-4}$ and 1 g cm$^{-3}$. The calculations represented by the solid lines include the equilibrating transitions. Dashed lines (that lie almost on top of the solid lines) were calculated using effective decay rates but no internal gamma transitions.

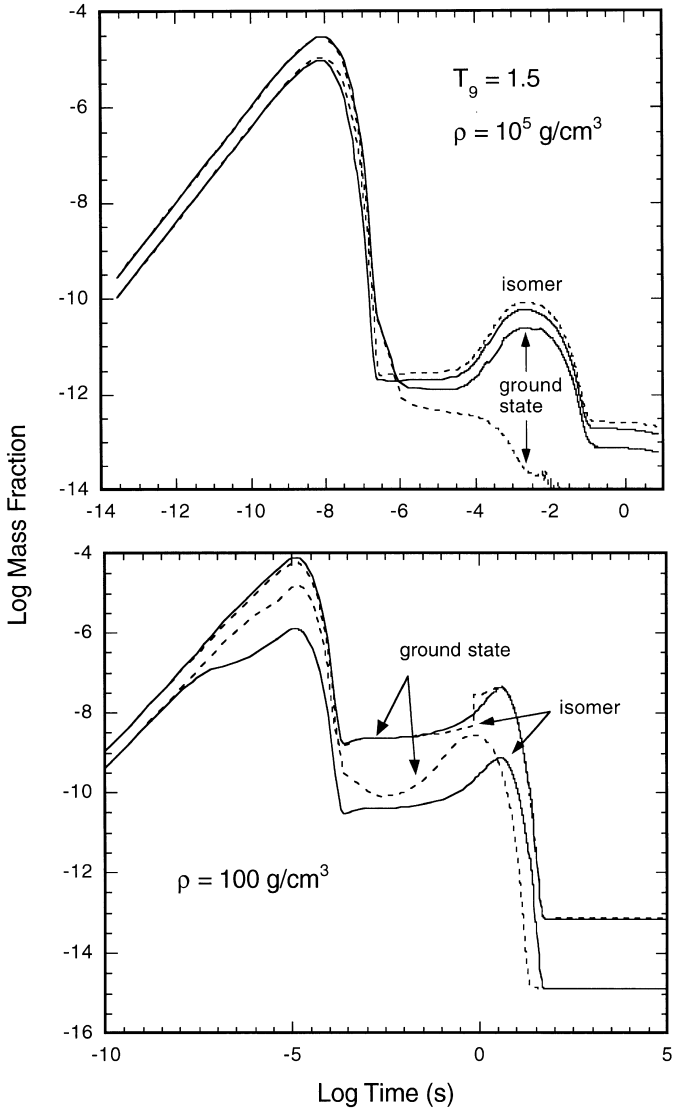


FIG. 9.—Same as Fig. 8, but for $T_9 = 1.5$, and $\rho = 100$ and $1 \times 10^5$ g cm$^{-3}$.

The results for $T_9 = 0.3$ (Fig. 8) show some aspects of the behavior that we described above. For both densities, $\tau_{nuc} = \tau_\beta^m < \tau_{eq}$, and so the system exhibits quasi-equilibrium behavior. It is possible to account for the abundance of the ground state by using an effective decay rate $\lambda_{eff}$ (from Fig. 2), although it should be noted that hydrogen exhaustion occurs before $\tau_{eff} = \lambda_{eff}^{-1}$. From a *numerical* standpoint, $^{26}$Al can be treated as separate nuclei, as advocated by WF and CPN. However, the proper $\tau_{eff}$ would have to be used (as suggested by CPN) if the calculation were run to longer times, and so from a *physical* standpoint, the two states are linked.

Very different behavior is apparent for $T_9 = 1.5$ (Fig. 9), where the use of an effective decay rate does not reproduce either the equilibrium or quasi-equilibrium abundances of the ground state. At this temperature and at both densities, the rate of the $^{25}$Al$(p, \gamma)^{26}$Si is faster than the $\beta^+$-decay of $^{25}$Al. This leads to a substantial quantity of $^{26}$Si, which in turn decays to the isomer. Here the production of the

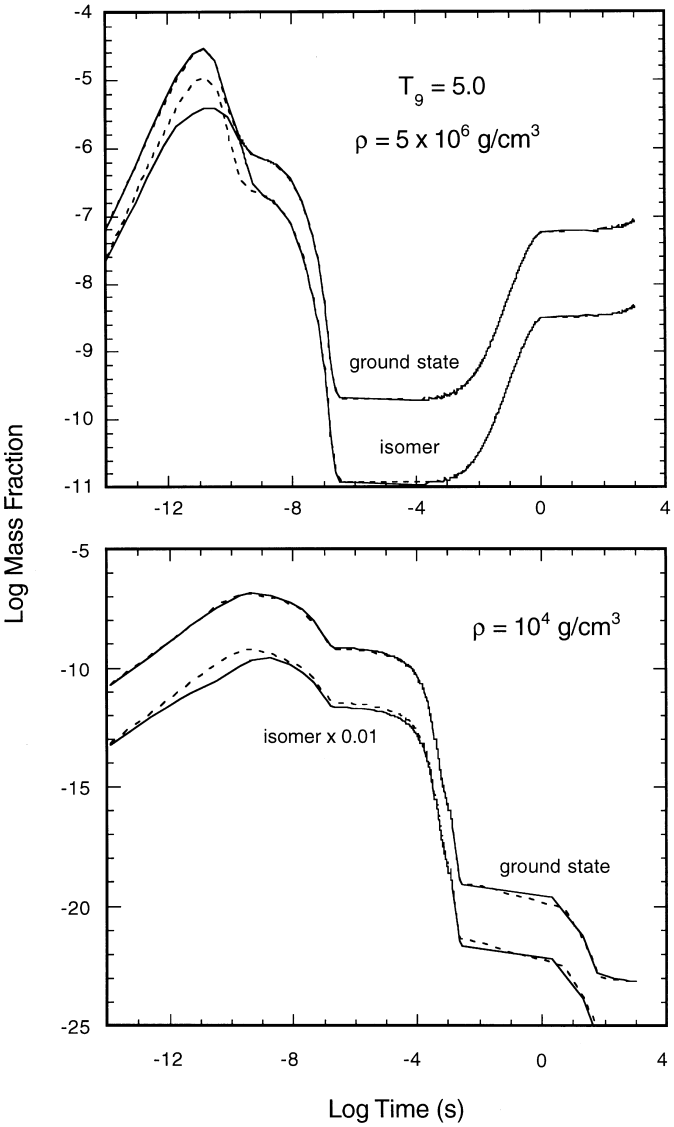


FIG. 10.—Same as Fig. 8, but for $T_9 = 5$, and $\rho = 1 \times 10^4$ and $5 \times 10^6$ g cm$^{-3}$.

isomer is now greatly enhanced with respect to the ground state. In thermal equilibrium, the ground state is 64 times more abundant than the isomer, and so equilibration converts the initially more abundant isomer into the ground state. Because production of $^{26}$Al favors the isomer, the gamma transitions linking the isomer with the ground state must be included in the network. At the higher of the two densities, $\tau_{eq} > \tau_{nuc}$ and a quasi-equilibrium with $m/g = 287$ (as opposed to the thermal ratio of 0.0156) is established. Equilibration is clearly an important effect; in both examples the majority of the ground-state production comes from thermal links with the isomer. However, in contrast to the general claims of WF for these temperatures, thermal equilibrium is not reached at the high density until hydrogen exhaustion increases $\tau_{nuc}$. At the lower density, the system does reach thermal equilibrium, in which 98% of the total abundance of $^{26}$Al is in the ground state. In both cases, $^{26}$Al is effectively produced by the $^{25}$Al($p$, $\gamma$)$^{26}$Si reaction, not by $^{25}$Mg($p$, $\gamma$)$^{26}$Al.

At $T_9 = 5$ (Fig. 10), the system returns to the situation where separate nuclei and effective decay rates do a very good job of describing the evolution of $^{26}$Al. This is because the extended MgAl cycle is again operating in a mode where production of the ground state exceeds that of the isomer. Although the chain $^{25}$Al($p$, $\gamma$)$^{26}$Si($\beta^+$)$^{26}$Al$^m$ is still operational, $^{26}$Al rapidly comes to a ($p$, $\gamma$)/($\gamma$, $p$) equilibrium with $^{25}$Mg and $^{27}$Si that favors production of the ground state over the isomer. At the higher density ($5 \times 10^6$ g cm$^{-3}$), this equilibrates $^{26}$Al faster than the internal transitions, so $\tau_{nuc} = \tau_{eq}$ and the system reaches thermal equilibrium. On the other hand, for $\rho = 1 \times 10^4$ g cm$^{-3}$, $^{26}$Al equilibrates internally, but rapid destruction via ($\gamma$, $p$) reactions results in a quasi-equilibrium with $^{25}$Mg. Once the ($p$, $\gamma$) reactions freeze out, the system will evolve to thermal equilibrium, which again can be described in terms of an effective decay rate.

## 5. CONCLUSION

In this paper, we have described the equilibration of $^{26}$Al in a manner analogous to that of a two-level system, with an effective decay rate described by equation (13). This expression is rather cumbersome, so the effective decay rate is displayed in tabular form in Table 2. We have also shown that there is no simple criterion that can be employed to determine if (or when) $^{26}$Al will reach thermal equilibrium. For $T_9 \leq 0.46$, $\tau_{eq} > \tau_{nuc}$ and the ground state and isomer reach a quasi-equilibrium in which $m/g$ is a constant but is less than the thermal ratio. At higher temperatures, thermal equilibrium will be reached only if $\tau_{eq} < \tau_{nuc}$. It is not immediately clear if this condition can be met in a highly dynamic situation.

As long as nuclear reactions produce $m/g < 1$, the evolution of $^{26}$Al can be calculated to good accuracy (i.e., better than 20%) by using an effective decay rate and ignoring the gamma transitions linking the ground state and isomer. This is true for both quasi-equilibrium and equilibrium conditions. However, the production of $^{26}$Si leads to $m/g > 1$, and therefore this simple approach breaks down when the abundance of $^{26}$Si becomes appreciable. This situation will manifest itself in hydrogen-rich environments at $T_9 \gtrsim 0.4$ (depending on density). However, for $T_9 \gtrsim 3$, equilibrium

TABLE 2

EFFECTIVE DECAY RATE OF $^{26}$Al

| $T_9$ | $\lambda_{eff}^a$ | $T_9$ | $\lambda_{eff}$ | $T_9$ | $\lambda_{eff}$ |
|---|---|---|---|---|---|
| 0.01000..... | 2.969E−14 | 1.30 | 1.278E−03 | 3.30 | 4.468E−03 |
| 0.0200..... | 2.969E−14 | 1.40 | 1.473E−03 | 3.40 | 4.602E−03 |
| 0.0500..... | 2.969E−14 | 1.50 | 1.665E−03 | 3.50 | 4.736E−03 |
| 0.0800..... | 2.969E−14 | 1.60 | 1.853E−03 | 3.60 | 4.869E−03 |
| 0.100..... | 2.969E−14 | 1.70 | 2.036E−03 | 3.70 | 5.001E−03 |
| 0.165..... | 3.706E−14 | 1.80 | 2.214E−03 | 3.80 | 5.132E−03 |
| 0.180..... | 1.145E−13 | 1.90 | 2.388E−03 | 3.90 | 5.262E−03 |
| 0.200..... | 1.276E−12 | 2.00 | 2.556E−03 | 4.00 | 5.391E−03 |
| 0.250..... | 1.572E−10 | 2.10 | 2.721E−03 | 4.10 | 5.519E−03 |
| 0.300..... | 4.287E−09 | 2.20 | 2.880E−03 | 4.20 | 5.647E−03 |
| 0.350..... | 1.520E−07 | 2.30 | 3.037E−03 | 4.30 | 5.773E−03 |
| 0.400..... | 5.595E−06 | 2.40 | 3.190E−03 | 4.40 | 5.899E−03 |
| 0.500..... | 4.932E−05 | 2.50 | 3.340E−03 | 4.50 | 6.024E−03 |
| 0.600..... | 1.204E−04 | 2.60 | 3.487E−03 | 4.60 | 6.148E−03 |
| 0.700..... | 2.261E−04 | 2.70 | 3.632E−03 | 4.70 | 6.270E−03 |
| 0.800..... | 3.624E−04 | 2.80 | 3.775E−03 | 4.80 | 6.392E−03 |
| 0.900..... | 5.226E−04 | 2.90 | 3.917E−03 | 4.90 | 6.513E−03 |
| 1.00..... | 6.998E−04 | 3.00 | 4.057E−03 | 5.00 | 6.633E−03 |
| 1.10..... | 8.880E−04 | 3.10 | 4.195E−03 | | |
| 1.20..... | 1.082E−03 | 3.20 | 4.332E−03 | | |

[a] Obtained from eq. (13).

between $^{26}$Al and $^{27}$Si again leads to $m/g > 1$, and the effective rate can again be used.

Finally, we would like to point out that the rate of the $^{25}$Al($p$, $\gamma$)$^{26}$Si is based on theoretical estimates (Iliadis et al. 1996) and is uncertain by a factor of about 100. Since this reaction plays an important role in the nucleosynthesis of $^{26}$Al at high temperatures, an experimental investigation of this reaction is called for.

We would like to thank C. Iliadis, B. S. Meyer, and D. D. Clayton for their helpful suggestions and W. E. Ormand for assistance with *oxbash*. One of us (A. E. C.) would also like to thank Mad Hatter's Bake Shop for their help in preparing this manuscript. This work was supported in part by the US Department of Energy under contracts DE-FG02-97ER41041 and DE-FG02-97ER41019.

## REFERENCES

Angulo, C., et al. 1999, Nucl. Phys. A, 656, 3
Brown, B. A., Etchegoyen, A., & Rae, W. D. M. 1988, The Computer Code *oxbash*, MSU-NSCL 524
Brown, B. A., Massen, S. E., Chung, W., Wildenthal, B. H., & Shibata, T. 1980, Phys. Rev. C, 22, 842
Carchidi, M., Wildenthal, B. H., & Brown, B. A. 1986, Phys. Rev. C, 34, 2280
Coc, A., Porquet, M.-G., & Nowacki, F. 1999, Phys. Rev. C, 61, 015801
Endt, P. M. 1990, Nucl. Phys. A, 521, 1
Iliadis, C., Buchmann, L., Endt, P. M., Herndl, H., & Wiescher, M. 1996, Phys. Rev. C, 53, 475
Iliadis, C., D'Auria, J. M., Starrfield, S., Thompson, W. J., & Wiescher, M. 2001, ApJS, 134, 151
Kajino, T., Shiino, E., Toki, H., Brown, B. A., & Wildenthal, B. H. 1988, Nucl. Phys. A, 480, 175
Knödlseder, J. 1999, ApJ, 510, 915
Knödlseder, J., et al. 1999, A&A, 345, 813
Prantzos, N., & Diehl, R. 1996, Phys. Rep., 267, 1
Warburton, E. K. 1992, Phys. Rev. C, 45, 463
Ward, R. A., & Fowler, W. A. 1980, ApJ, 238, 266
Wildenthal, B. H. 1984, Prog. Part. Nucl. Phys., 11, 5